Special Issue

Multimodal Imaging of Macular Telangiectasia Type 2: Focus on Vascular Changes Using Optical Coherence Tomography Angiography

Lisa Toto,[1] Luca Di Antonio,[1] Rodolfo Mastropasqua,[2] Peter A. Mattei,[1] Paolo Carpineto,[1] Enrico Borrelli,[1] Marco Rispoli,[3] Bruno Lumbroso,[3] and Leonardo Mastropasqua[1]

[1]Department of Medicine and Science of Aging, Ophthalmology Clinic, University "G. d'Annunzio" Chieti-Pescara, Chieti, Italy
[2]Ophthalmology Clinic, University of Verona, Verona, Italy
[3]Italian Macular Center, Rome, Italy

Correspondence: Lisa Toto, Clinica Oftalmologica, Ospedale Clinicizzato, Via Dei Vestini 31, Chieti, Italy; l.toto@unich.it.

Submitted: December 13, 2015
Accepted: March 13, 2016

LT and LDA contributed equally to the work presented here and should therefore be regarded as equivalent authors.

Citation: Toto L, Di Antonio L, Mastropasqua R, et al. Multimodal imaging of macular telangiectasia type 2: focus on vascular changes using optical coherence tomography angiography. *Invest Ophthalmol Vis Sci*. 2016;57:OCT268–OCT276. DOI:10.1167/iovs.15-18872

Purpose. To report morphologic features of idiopathic macular telangiectasia (MacTel) type 2 by means of optical coherence tomography angiography (OCTA) and to compare these findings to fundus fluorescein angiography (FFA), fundus autofluorescence (FAF), confocal blue reflectance (CBR), and spectral-domain OCT (SD-OCT). In addition, foveal vessel density and parafoveal vascular density (PFVD), and foveal retinal thickness and parafoveal retinal thickness (PFRT) were compared between MacTel 2 patients and normal aged-matched controls.

Methods. Eight patients (15 eyes) with MacTel 2 and 17 normal controls (17 eyes) underwent retinal multimodal imaging assessment and grading. Results from different imaging techniques were used to compare interimaging modalities. Objective quantification of retinal vessel density and macular thickness was evaluated in MacTel 2 patients (15 eyes).

Results. In MacTel 2 eyes a comparison of OCTA to the other imaging techniques showed that the strongest correlations were present with SD-OCT, early FFA, and late FFA. Moderate correlations were found between OCTA and CBR and FAF. Foveal vessel density was significantly lower in MacTel 2 eyes than control eyes both in the superficial plexus (23.74% vs. 33.14%; $P = 0.003$) and in the deep plexus (24.63% vs. 34.21%; $P = 0.005$). Superficial PFVD was significantly different in the two groups (47.06% vs. 51.40%; $P = 0.005$) but not the deep PFVD. Foveal retinal thickness was 214.13 μm in MacTel 2 eyes and 258.18 μm in normal controls, and PFRT was 279.60 and 323.29 μm, respectively ($P < 0.0001$).

Conclusions. Optical coherence tomography angiography is useful for retinal vasculature characterization in MacTel type 2 patients and showed a high correlation with well-established imaging techniques.

Keywords: optical coherence tomography angiography, fluorescein angiography, macular telangiectasia

Idiopathic macular telangiectasia (MacTel) refers to retinal capillary ectasia limited to the perifoveal area without a specific cause. This entity was originally classified by Gass and Oyakawa[1] in 1982. In 1993 the classification was revised by Gass and Blodi,[2] and further simplified by Yannuzzi et al.[3] in 2006. Currently, MacTel is classified into two categories mainly by biomicroscopic and fluorescein angiographic features.

Idiopathic macular telangiectasia type 2 (perifoveal telangiectasia) is a bilateral disease that affects men and woman, starting in the fifth to seventh decades of life. Early manifestations of the disease include loss of retinal transparency, superficial retinal crystalline deposits, right-angled venules, and presence of intraretinal cystoid spaces in the fovea. In later stages, the intraretinal pigment migrates, forming pigment plaques, and subretinal neovascular membrane develops.

Fundus fluorescein angiography (FFA) has been considered for many years the gold standard for diagnosis of MacTel type 2. The classic FFA finding is telangiectatic vessels that leak dye in the parafoveal area with fluorescein leakage not related to the cystic spaces.[4]

In recent years spectral-domain optical coherence tomography (SD-OCT) has shown neurodegenerative changes of MacTel 2, including presence of hyporeflective spaces in the inner or outer retina, foveal thinning, intraretinal pigments, and foveal detachment. In some advanced cases, serous retinal detachment with subretinal new vessels above the level of the RPE may be seen.[4]

Blue-light fundus autofluorescence (FAF), used as a complementary tool for MacTel 2 diagnosis, shows an increase of relative hyperautofluorescence in the temporal perifoveal area due to macular pigment depletion in early stages, with vascular alterations extending centripetally and a more diffuse, circumferential relative increase in autofluorescence as the disease progresses. In the late phases, in the presence of retinal pigment epithelium (RPE) atrophy, areas of hypoautofluorescence are visible, coupled with increased relative hyperautofluorescence.[4,5]

Table 1. Fundus Autofluorescence Grading

Grade	Characteristics
1	Absence of foveal central depression of autofluorescence
2	Higher-than-expected signal in the fovea (ranging from a mild increase obscuring the foveal depression to slightly exceeding the parafoveal regions)
3	Heterogeneous pattern of autofluorescence (increased and decreased fundus autofluorescence signal)

Since the first classification of MacTel 2 by Gass et al.,[1,2] which was mainly based on clinical and angiographic findings, several classifications have been proposed. The most recent is based on multimodality imaging using FFA, FAF, and OCT findings.[4–6]

Recently, Spaide at al.[7] have reported findings on OCT angiography (OCTA) using the Split-Spectrum Amplitude Decorrelation Algorithm (SSADA) of patients affected by MacTel type 2. They observe qualitative alterations in both the superficial and deep plexus.[7] These alterations include loss of capillaries, dilation and telangiectasis, and new vessels in the outer and subretinal spaces.

The purpose of this study was to report the morphologic features of MacTel type 2 observed with OCTA and to correlate these findings to those obtained with well-established imaging techniques such as FFA, FAF, confocal blue reflectance (CBR), and SD-OCT. In addition we compared vessel density and macular thickness in MacTel type 2 patients and normal age-matched controls.

Methods

The study adhered to the tenets of the Declaration of Helsinki and was approved by the Institutional Review Board. Informed consent was obtained from all patients before their enrollment.

Eight patients (15 eyes) with previous clinical and FFA diagnosis of MacTel type 2 and 17 normal age-matched controls (17 eyes) were enrolled at the Retina Service of the Ophthalmology Clinic, University "G. d'Annunzio" in Chieti-Pescara, Italy.

Inclusion criteria for the patient group were all eyes with either nonproliferative or proliferative MacTel type 2. Eyes with any other retinal pathology, including diabetic retinopathy, retinal vein occlusion, choroidal neovascularization secondary to age-related macular degeneration, a history of any prior vitreoretinal surgery or of photodynamic therapy, were excluded from the study.

All patients and controls underwent a comprehensive ophthalmologic examination, including measurements of best-corrected visual acuity (BCVA), intraocular pressure, fundus examination, and OCTA imaging (XR Avanti; Optovue, Inc., Fremont, CA, USA). Patients underwent scanning of both eyes and controls underwent examination of the enrolled eye with OCTA. Each patient with MacTel type 2 underwent color fundus photography, FAF, FFA, CBR, and SD-OCT.

Table 2. Confocal Blue Reflectance Grading

Grade	Characteristics
1	Increased parafoveal reflectance limited to two temporal quadrants
2	Increased parafoveal reflectance limited to three quadrants including the temporal quadrants
3	Ring-like area of increased parafoveal reflectance

Table 3. Early-Phase (10–20 Seconds) Fundus Fluorescein Angiography Grading

Grade	Characteristics
1	Temporal changes
2	Temporal and nasal changes
3	Full involvement
4	Any previous grade with signs of NV similar to classic NV characterized by hyperfluorescence

NV, neovascularization.

Color fundus photographs of the optic disc, macula, and temporal retina (30° field of view) were acquired with Navilas instrument (NAVILAS; OD-OS, Teltow, Germany).

The Heidelberg Retina Angiograph 2 (HRA2) with confocal scanning laser ophthalmoscope (HRA+OCT Spectralis; Heidelberg Engineering, Heidelberg, Germany) was used for FAF imaging with an excitation wavelength of 488 nm and a barrier filter at 500 nm. Fundus autofluorescence categories of MacTel type 2 patients were graded as previously described by Wong et al.[5] (Table 1).

Confocal blue reflectance was performed by using HRA2 with an excitation wavelength of 488 nm and classified into three grades (Table 2).

Fundus fluorescein angiography was performed with a HRA2 by using the routine FFA procedure with a 5-mL intravenous injection of 10% sodium fluorescein solution. One representative image of early-phase (10–20 seconds) angiogram and one image of the late phase (10 minutes) were graded for each patient as previously described for the nonproliferative stages.[6] Early FFA was graded according to the extent of changes such as dilated retinal capillaries, telangiectatic vessels, and dilated blunted right-angled veins. Late FFA was graded according to the same pattern as early-FFA changes. Categories were defined by using the foveal center as the main landmark. For proliferative stages an additional grade was defined (Tables 3 and 4).

Spectral-domain OCT volume of the retina was acquired with a Heidelberg Spectralis OCT system. The retinal area of a volume scan covered a field of view of $20 \times 20°$ acquired with at least 49 B-scans per volume. Optical coherence tomography alterations were classified as previously described (Table 5).[6]

Grading of each imaging technique was performed independently by two retinal experts and results were compared for interobserver reliability. Subsequently, final grading was determined in consensus and these results were used to compare interimaging modality.

Imaging With XR Avanti

XR Avanti SD-OCT offers high speed (70,000 axial scans per second) with an 840-nm light source and an axial resolution of 5 um. Pupils were dilated before acquisitions, with a combination of 1% tropicamide and 2.5% phenylephrine.

Table 4. Late-Phase (10 Minutes) Fundus Fluorescein Angiography Grading

Grade	Characteristics
1	Temporal changes
2	Temporal and nasal changes
3	Full involvement
4	Any previous grade with an increase in intensity and size, presence of membrane or hypofluorescence due to subretinal hemorrhage

Table 5. Optical Coherence Tomography Grading

Grade	Characteristics
1	A break in the IS/OS junction line, as well as the inner and smaller outer retinal cysts, confined to the temporal side of the foveal center
2	A larger break in the IS/OS that reaches the foveal center, central outer cysts, and inner cysts involving also the nasal area, temporal side, with the retinal layers disorganized; the outer plexiform layer and the layers internal to it extend toward the choroid ("collapsing layers"). Hyperreflective intraretinal lesion due to pigment plaques is visible.
3	Only minor retinal cysts remain, the IS/OS break involves the nasal and the temporal area center, and the "collapse" of the layers is extensive. Hyperreflective intraretinal lesion due to pigment plaques is visible.
4	Any of the signs of grade 1 to 3 with signs of NV similar to classic NV characterized by hyperreflective lesion located in, or external to, the outer neurosensory retinal layers associated to subretinal or intraretinal fluid

The AngioVue software (version 2015.100.0.35; Optovue, Inc.) used in this study was a prerelease version implementing SSADA. This algorithm uses flow as the intrinsic contrast, detecting the variation over time in the speckle pattern formed by interference of light scattered from moving red blood cells and adjacent stationary tissue structures.[8,9]

Study participants underwent SD-OCT imaging following a protocol that included AngioVue OCT 3D volume set at 3 × 3 mm, consisting of 304 × 304 pixels in the transverse dimension. An internal fixation light was used to center the scanning area.

One FastX (horizontal raster) set and one FastY (vertical raster) set were performed for each acquisition scan. Scans with low quality (i.e., if the subject blinked or if there were many motion artifacts in the data set) were excluded and repeated until good quality was achieved. The user can manually fine-tune the plane to maximize the visualization of the retinal capillary bed. Three angiography scans of best quality were considered for analysis.

Vascular retinal layers were visualized and segmented as previously described.[7] To evaluate the superficial retinal plexus, we used a layer thickness of 60 μm from the inner limiting membrane, in order to include all the vessels of this plexus. Therefore, to visualize the deep retinal plexus, we used a 30-μm-thick layer from the inner plexiform layer, for the purpose of visualizing the plexus in its entirety. To remove projection artefacts from the inner vascular plexus, the slab section was moved slightly posteriorly and centered on the outer plexifom layer. The outer retina is from the outer nuclear layer to the Bruch's membrane and was used to visualize eventual subretinal neovascularization. The software option to remove projection artefacts from the inner vascular plexus in the outer retina was selected.

Qualitative Vessel Analysis

Two independent observers subjectively evaluated OCTA in the 3 × 3-mm scan of best quality. Optical coherence tomography angiography was graded according to the lateral extension of vascular anomalies, using the foveal center as the main landmark: OCTA grade 1, vascular anomalies in the deep and/or superficial plexus temporal to the fovea; OCTA grade 2, vascular anomalies in the deep and/or superficial plexus temporal and nasal to the fovea; OCTA grade 3, markedly diffuse circumferentially vascular anomalies in the deep and superficial plexus; and OCTA grade 4, neovascularization in the outer retina with any OCTA signs of grade 1 to 3 (Fig. 1; Table 6).

Table 6. Optical Coherence Tomography Angiography Grading

Grade	Characteristics
1	Vascular anomalies in the deep and/or superficial plexus temporal to the fovea
2	Vascular anomalies in the deep and/or superficial plexus temporal and nasal to the fovea
3	Markedly diffuse circumferential vascular anomalies in the deep and superficial plexus
4	Neovascularization in the outer retina with any OCTA signs of grade 1 to 3

Vascular anomalies were evaluated in terms of vessel caliper (regular or irregular such as telangiectatic vascular abnormalities and/or microaneurysm), vessel coarse irregularities (regular or irregular such as distorted or right angled), and vessel density (normal or rarified).

Quantitative Vessel Analysis

Objective quantification vessel density was evaluated with OCTA en face images for each eye by using the AngioVue software. The flow area was calculated with a user-defined circular region of interest (ROI) and a threshold. The area within the ROI with intensities greater than the threshold was calculated. The vessel density was defined as the percentage area occupied by vessels in a circular ROI centered on the center of the foveal avascular zone and with a diameter of 2.5 mm. The AngioVue software automatically splits the ROI into the following two fields: the foveal area, a central circle with a diameter of 1 mm; and the parafoveal area that constitutes the remaining part inside the ROI.

The AngioVue software automatically outputs the vessel density percentage inside the foveal area (foveal vessel density – FVD), in the whole parafoveal area (parafoveal vessel density – PFVD), and in different quadrants of the parafoveal area (temporal, superior, nasal, and inferior).

The vessel density is calculated by using the formula previously described,[8] as follows:

$$\text{Vessel density} = \frac{\int V \cdot dA}{\int dA},$$

where V is 1 when the OCTA value is above a background threshold, and 0 otherwise. A is the area of interest.

Enhancement of Vessel Detection

To facilitate the visualization of the outer and inner retinal plexus and to highlight the presence of outer retinal vessel proliferations, the inner retinal vessels were colored violet, deep retinal vessels blue, and the neovascularization green. This was done by using the 3D spot segmentation with the Watershed option in ImageJ (http://imagej.nih.gov/ij/; provided in the public domain by the National Institutes of Health, Bethesda, MD, USA).

Foveal and Parafoveal Retinal Thickness Analysis

Foveal and parafoveal retinal thickness in different retinal quadrants were automatically calculated by the software on the OCTA 3 × 3-mm volume scan (XR Avanti). A circular ROI

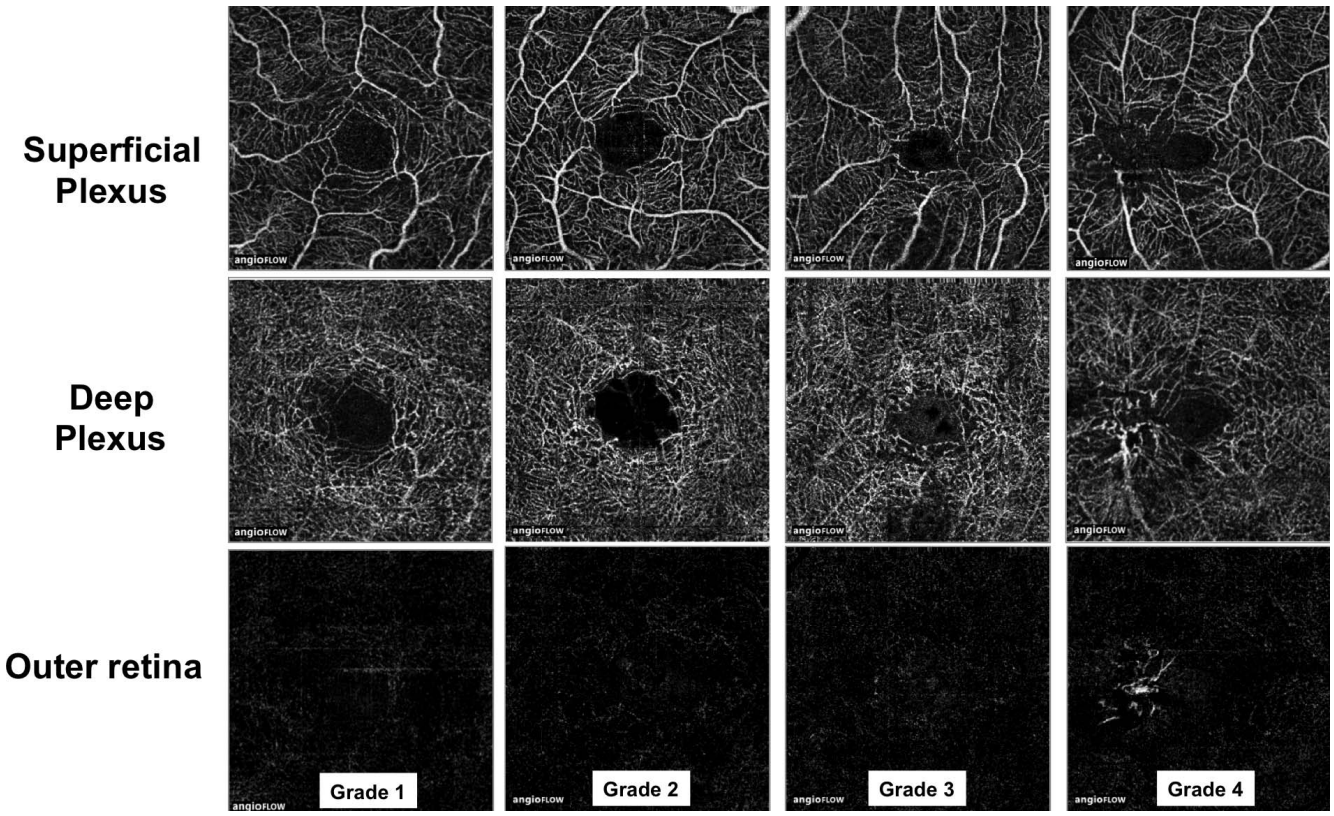

FIGURE 1. Optical coherence tomography angiography in MacTel type 2 patients, showing anomalies in the superficial plexus, deep plexus, and outer retina from grade 1 to 4. Optical coherence tomography angiography grade 1 of a left eye: vascular anomalies temporal to the fovea consisting of telangiectatic and somewhat rarified vessels in the deep plexus temporal to the fovea and somewhat rarified vessels in the superficial plexus temporal to the fovea. Optical coherence tomography angiography grade 2 of a right eye: vascular anomalies in the deep and superficial plexus temporal and nasal to the fovea, mainly represented by rarified and telangiectatic vessels in the deep plexus temporal and nasal to the fovea and rarified and somewhat telangiectatic vessels in the superficial temporal plexus and slightly rarified vessels in the superficial nasal plexus. Optical coherence tomography angiography grade 3 of a left eye: markedly diffuse circumferential vascular anomalies with telangiectatic, rarified, and distorted vessels in the deep and superficial plexus. Optical coherence tomography angiography grade 4 of a right eye: signs of neovascularization in the outer retina associated with markedly diffuse vascular anomalies in the superficial and deep plexus.

centered on the center of the foveal avascular zone with a diameter of 2.5 mm was considered for retinal thickness analysis: central foveal area (1 mm in diameter) and the parafoveal area that constitutes the remaining part inside the ROI (total parafoveal area or temporal, superior, nasal, and inferior quadrants).

Statistical Analysis

All statistical analyses were evaluated at an α level of 0.05, false discovery rate (FDR) corrected for multiple testing. Statistical analysis was performed with SPSS 22.0 (IBM, Armonk, NY, USA).

Depending on the type of data to be analyzed, parametric (paired t test) or nonparametric (McNemar, Wilcoxon sign rank, and Mann-Whitney) tests were used to compare patient characteristics at the time of enrollment, vessel density, and macular thickness. Statistically significant differences in interobserver and interimaging modality concordance were determined by using linear-weighted Cohen's κ and Spearman's rank correlation coefficient, corrected for multiple testing using the FDR. Spearman correlation coefficient is not based on the distribution of the two variables, but on their ranks, and expresses the strength of linkage or co-occurrence between two variables in a single value between −1 (negative correlation) and +1 (positive correlation). Statistical analysis was performed with MedCalc (version 15.2; MedCalc Software, Ostend, Belgium).

RESULTS

Demographic Data

The mean age ± SD was 67.27 ± 4.92 years (range, 61–76 years) for patients with MacTel 2 and 65.76 ± 6.75 years (range, 59–83 years) for the control group. The difference in age between the two groups was not statistically significant ($P = 0.483$). Twelve eyes in the MacTel 2 group and 14 eyes in the control group were from women ($P = 1.000$; χ^2 test); the mean BCVA was 0.50 ± 0.17 logMAR and 0.02 ± 0.10 logMAR, respectively ($P = 0.0001$; Mann-Whitney U test).

Patient Population

Fluorescein angiography imaging was not performed in one patient due to an allergy to fluorescein dye. Optical coherence tomography angiography data were of poor quality form one eye of a patient with low vision.

Morphologic Features in MacTel Type 2 Patients by OCTA

Optical coherence tomography angiography provided detailed images of the retinal microcirculation in all patients with MacTel type 2. In these patients, the microvascular network of the macular region was visible on OCT angiograms and showed

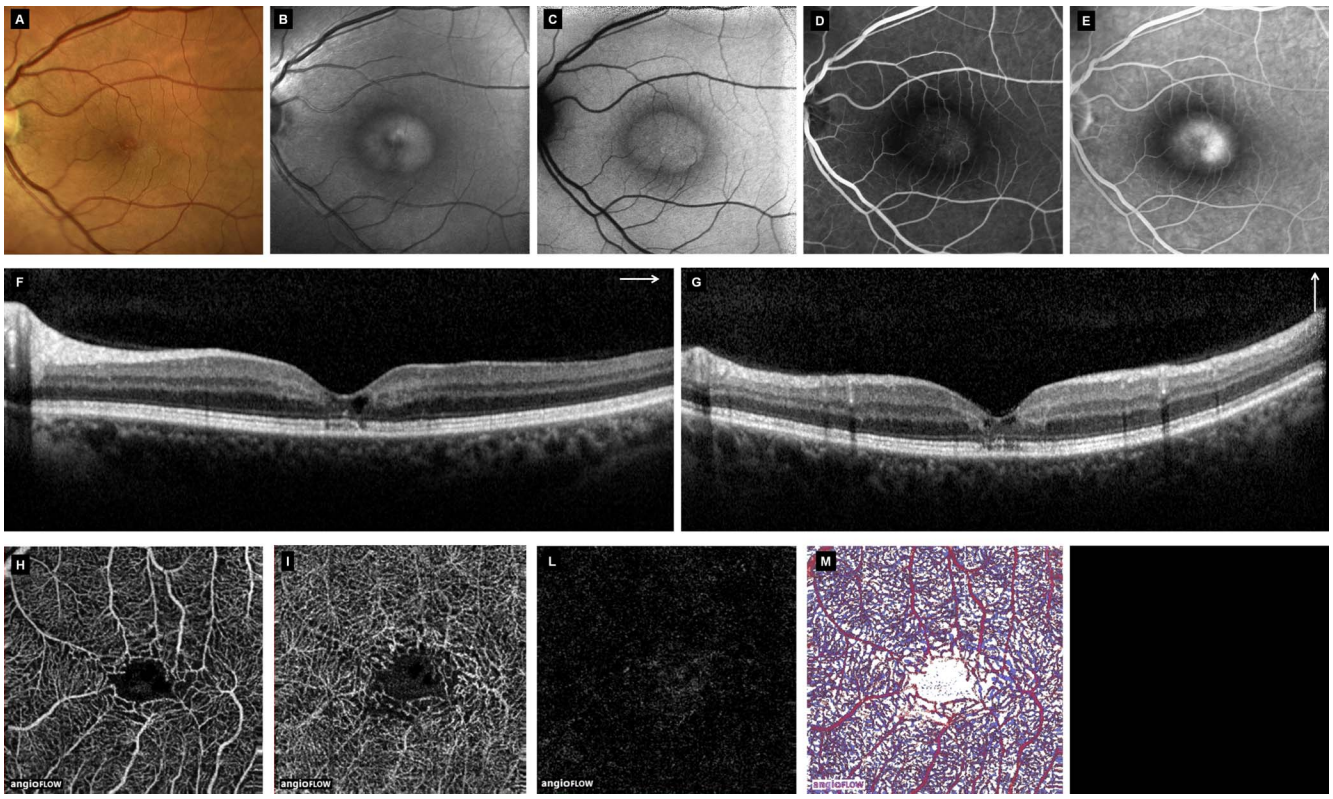

FIGURE 2. Multimodal imaging of a patient with MacTel type 2 in a nonproliferative stage. Fundus photography (**A**) showing parafoveal loss of retinal transparency mainly located temporally to the fovea; CBR (**B**) demonstrating a ring-like area of increased parafoveal reflectance; mild increase of foveal autofluorescence obscuring the foveal depression with patchy hyperautofluorescence slightly exceeding the parafoveal regions on FAF (**C**); early (**D**) and late (**E**) FFA revealing full macular involvement with early hyperfluorescence due to telangiectatic vessels and leakage in the late phases; SD-OCT horizontal scan (**F**) and SD-OCT vertical scan (**G**) showing breaks of the IS/OS line and ELM line and inner and outer retinal cysts both in the temporal and nasal sides; OCTA showing markedly diffuse macular anomalies with telangiectatic, rarified, and somewhat distorted vessels of superficial plexus (**H**) and deep plexus (**I**) and no vessel proliferation in the outer retina (**L**); OCTA color image of the same plexuses (**M**). ELM, external limiting membrane; IS/OS, inner segment/outer segment.

several alterations in terms of vessel caliper, such as diffuse or sectoral telangiectatic vessels, diffuse or sectoral rarified vessels, distorted vessels, and neovascularization.

In MacTel type 2 eyes, 1 (7%) of 15 eyes showed a grade-1 OCTA (Fig. 1); 6 eyes (40%) a grade 2; 5 eyes (33%) a grade 3 (Fig. 2A–M); and 3 eyes (20%) a grade 4 (Fig. 3A–M). The more prominent features in OCTA, independent of grade, were vessel ectasia, particularly evident in the deep plexus, and vessel rarefaction with increasing intervascular spaces involving the superficial and the deep plexus in the foveal region and mainly the superficial plexus in the parafoveal region. Vessel ectasia and rarefaction either in the superficial or the deep plexuses were detected in all eyes (100%).

Coarse irregularities of blood vessels, such as right-angle vessels, were particularly evident in 4 (27%) of 15 eyes with concomitant pigment plaques.

Three (20%) of 15 eyes showed neovascularization in the outer retina. The vessel proliferation was discernible only in one case (7%) with FFA; in another case, the diagnosis with FFA could not be made; and in the third case, FFA was not performed owing to an allergy to the dye.

Vessel Density Analysis

Foveal vessel density and PFVD of the superficial plexus were significantly lower in MacTel 2 group than in the control group (23.74% vs. 33.14%, $P = 0.003$; and 47.06% vs. 51.40%, $P = 0.005$). Parafoveal vascular density was significantly lower in all quadrants in MacTel 2 group than in the control group (Table 7).

Foveal vessel density of the deep plexus was significantly lower in MacTel 2 group than in the control group (24.63% vs. 34.21%; $P = 0.005$). Parafoveal vascular density in the deep plexus was not significantly different between the two groups (57.68% vs. 57.61%; $P = 0.947$), nor were there significant differences in any quadrant (Table 7).

Macular Thickness Analysis

Foveal retinal thickness was 214.13 μm in MacTel 2 eyes and 258.18 μm in normal controls, and PFRT was 279.60 and 323.29 μm, respectively ($P < 0.0001$). Parafoveal retinal thickness in all quadrants was significantly different between the two groups (Table 8).

Interreader Agreement

The degree of interreader agreement was excellent for early FFA, SD-OCT, OCTA, CBR, and FAF, while it was only strong for late FFA (Table 9).

Multimodal Imaging Features

Macular alterations on FAF, FFA, CBR, and SD-OCT were observed in all patients with MacTel 2.

In 4 (27%) of 15 eyes, a grade-1 FAF alteration was present, in 5 (33%) a grade 2 FFA, and in 6 (40%) a grade 3.

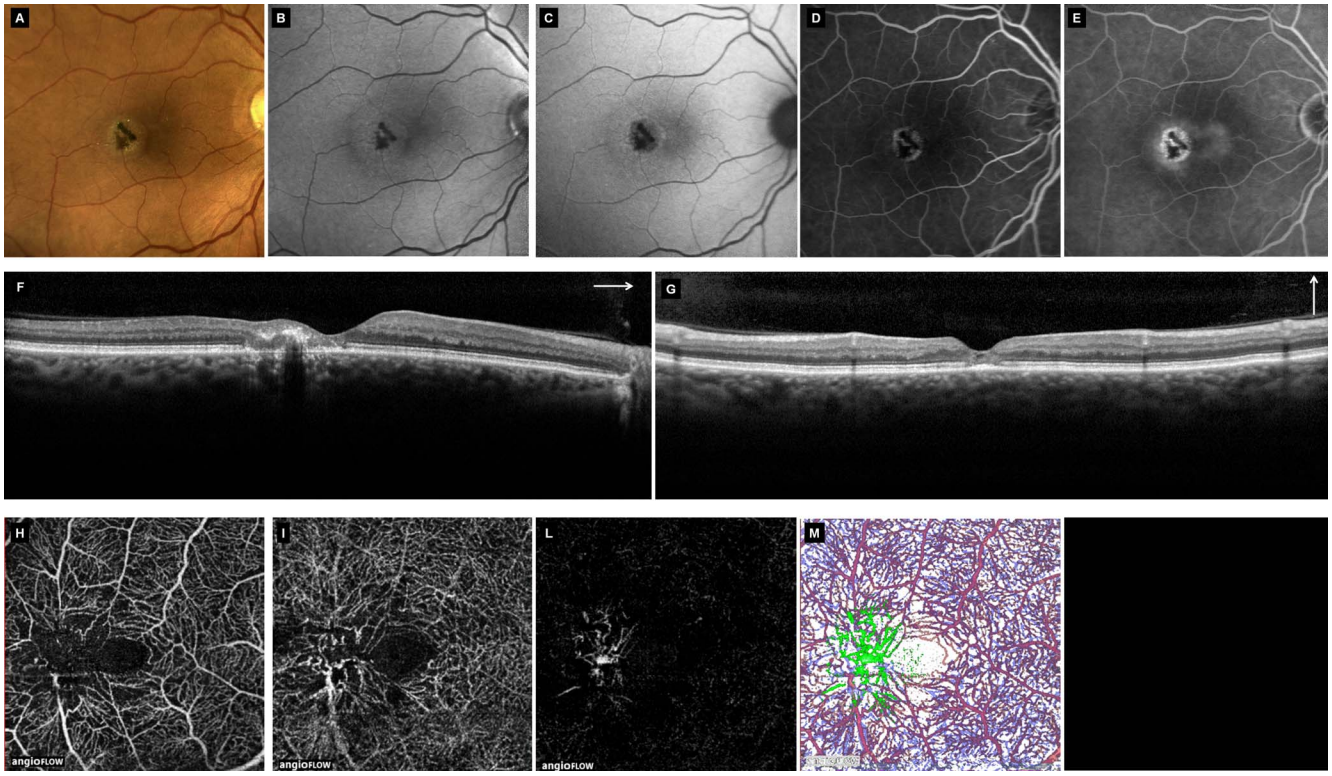

FIGURE 3. Multimodal imaging of a patient with MacTel type 2 in a proliferative stage. Fundus photography (**A**) showing foveal pigment clumps with perilesional loss of retinal transparency. Confocal blue reflectance (**B**) demonstrating a ring-like area of increased parafoveal reflectance surrounding the pigment clump. Increased and decreased autofluorescence signals are visible on FAF (**C**). Early FFA (**D**) reveals an early subfoveal hyperfluorescence with leakage in the late phases (**E**) due to intraretinal neovascularization surrounded by an annular area of hypofluorescence due to the pigment clump and an external parafoveal hyperfluorescence due to telangiectatic vessels and epithelial pigment atrophy with leakage in the late phases; SD-OCT horizontal scan (**F**) shows hyperreflective lesion in the outer retina and a break of the IS/OS and ELM lines, and SD-OCT vertical scan (**G**) shows break of the IS/OS and ELM lines and inner retinal cysts; OCTA shows markedly diffuse macular anomalies with telangiectatic, rarified, and distorted vessels of superficial plexus (**H**) and deep plexus (**I**) and neovascular proliferation in the outer retina (**L**); OCTA color image showing the superficial plexus in *violet*, the deep plexus in *blue*, and the neovessel proliferation in *green* (**M**).

Early- and late-FFA grading was the same in all eyes with 4 (29%) eyes of 14 showing a grade 1; 9 (64%) eyes a grade 3; and 1 (7%) eye a grade 4.

Confocal blue reflectance showed a grade 1 in 5 (33%) eyes and a grade 3 in 10 (67%) eyes.

In 3 (20%) of 15 eyes, a grade-1 SD-OCT was present, in 8 (54%) a grade 2, in 2 (13%) a grade 3, and in 2 (13%) a grade 4.

All grade-3 FAF eyes showed full macular involvement or macular neovascularization features in early and late FFA (grade 3 or 4). Ten (67%) of 15 eyes with different FAF grades (from 1

TABLE 7. Foveal and Parafoveal Vessel Density of the Superficial and Deep Plexuses Evaluated by OCTA in MacTel 2 Group and Control Group

	MacTel 2 Group, $n = 15$ Eyes				Control Group, $n = 17$ Eyes			
	Foveal Superficial Vessel Density, %	Foveal Deep Vessel Density, %	Parafoveal Superficial Vessel Density, %	Parafoveal Deep Vessel Density, %	Foveal Superficial Vessel Density, %	Foveal Deep Vessel Density, %	Parafoveal Superficial Vessel Density, %	Parafoveal Deep Vessel Density, %
Total	23.74 ± 5.67*	24.63 ± 5.89*	47.06 ± 4.68*	57.68 ± 3.46	33.14 ± 9.99	34.21 ± 10.89	51.40 ± 3.33	57.61 ± 2.18
Temporal quadrant	NA	NA	44.57 ± 7.60†	56.57 ± 3.79	NA	NA	50.15 ± 4.01	55.85 ± 2.34
Superior quadrant	NA	NA	48.15 ± 4.31*	58.51 ± 3.72	NA	NA	52.18 ± 3.20	59.77 ± 3.44
Nasal quadrant	NA	NA	46.97 ± 5.33†	56.83 ± 4.02	NA	NA	51.03 ± 3.44	56.67 ± 2.66
Inferior quadrant	NA	NA	48.32 ± 5.22†	59.12 ± 3.56	NA	NA	52.23 ± 4.47	58.16 ± 2.90

NA, not applicable.

* $P < 0.01$; † $P < 0.05$; *t*-test for equality of means between MacTel 2 group and control group.

Table 8. Foveal and Parafoveal Thickness Evaluated by Means of Spectral OCT in the MacTel 2 Group and in the Control Group

	MacTel 2 Group, $n = 15$ Eyes		Control Group, $n = 17$ Eyes	
	Foveal Thickness, μm	Parafoveal Thickness, μm	Foveal Thickness, μm	Parafoveal Thickness, μm
Total	214.13 ± 28.16*	279.60 ± 15.67*	258.18 ± 21.42	323.29 ± 13.33
Temporal quadrant	NA	269.07 ± 30.16*	NA	313.35 ± 13.36
Superior quadrant	NA	279.73 ± 15.75*	NA	327.71 ± 15.30
Nasal quadrant	NA	287.93 ± 16.03*	NA	326.82 ± 14.63
Inferior quadrant	NA	281.07 ± 13.09*	NA	325.53 ± 12.06

* $P < 0.001$; *t*-test for equality of means between MacTel 2 group and control group.

to 3) showed full macular increased CBR (grade 3). Except for one patient (two eyes), all eyes with full macular involvement or signs of macular neovascularization in early and late FFA (grade 3 and 4) corresponded to full macular increased CBR (grade 3). On SD-OCT, two eyes were grade 4 and in one of the two eyes, neovascularization was discernible also with FFA (grade 4).

Comparison Imaging Modalities

A comparison of OCTA to the other imaging techniques showed that the strongest correlations were present with SD-OCT, early FFA, and late FFA. Moderate correlations were found with CBR and FAF (Table 10).

Comparing all imaging modalities, high correlations were found between CBR and early and late FFA. Moderate correlations were found between SD-OCT and early and late FFA and SD-OCT and CBR. A low correlation was found between FAF and CBR (Table 10).

Discussion

Angio-OCT is a new imaging technique providing visualization of the retinal and choroidal circulation with depth information. It allows for the ability to visualize and analyze separately the two main retinal vascular plexuses that cannot be distinguished by conventional imaging techniques such as FFA.[8,10–12] In more recent years, OCTA has been applied to the study of retinal vascular plexuses in retinal and optic nerve pathologies.[7,13,9]

Thorell et al.[13] were the first to study vessel alterations in MacTel type 2, using OCT-based microangiography. In 2015 Spaide et al.[7] used OCTA to image patients affected by MacTel type 2 and observed some loss of capillary density in the inner retinal vascular plexus with more prominent alterations in the deep retinal vascular plexus. The alterations range from dilation and telangiectasis in milder forms to thinning and loss in more advanced cases. New vessels are observed invading the outer and subretinal spaces subjacent to the regions showing greatest flow abnormalities in the inner and deep retinal vascular layers.[7]

Table 9. Interreader Comparison for Imaging Methods Evaluated With Linear Weighted Cohen's κ

	Weighted κ	95% CI	Agreement
FAF	0.835	0.0632–1.000	Excellent
Early FFA	1.000	1.000–1.000	Excellent
Late FFA	1.000	1.000–1.000	Excellent
SD-OCT	1.000	1.000–1.000	Excellent
CBR	1.000	1.000–1.000	Excellent
OCTA	1.000	1.000–1.000	Excellent

CI, confidence interval.

Recently, Zeimer et al.[14] have noted vascular alterations mainly characterized by reduction of the capillary network in the inner retinal vascular plexus and dilatation and telangiectasis in the deep plexus, associated with vascular proliferation of the outer retina. Zhang et al.[15] report better visualization of retinal vessel proliferation in MacTel 2 eyes when using OCTA rather than fluorescein angiography.

Optical coherence tomography angiography has also clarified correlations between capillary proliferation in the outer retina and ellipsoid zone loss.[16] Our study evaluated the utility of OCTA for visualizing and quantifying vessel alterations in MacTel type 2 and correlated these findings with other imaging modalities such as FFA, FAF, CBR, and SD-OCT. Optical coherence tomography angiography was performed in MacTel type 2 eyes and in healthy subjects by using a high-speed 840-nm wavelength SD-OCT XR Avanti with SSADA.

In all patients with MacTel type 2, OCTA detected blood vessel alterations at various depths and with a spatial distribution similar to that detected with other imaging techniques: starting at the temporal edge of the fovea and then progressing to the nasal retina up to the complete involvement of the perifoveal region in more advanced stages.[4,6] Ectasia of deep and superficial vessels was present in all eyes with more severe anomalies of the deep plexus than the superficial plexus.

Rarefaction of foveal vessel with an increase of the intervascular spaces was another common feature, detected in all eyes involving the superficial and deep plexus. In the parafoveal region a greater rarefaction was observed mainly in the superficial plexus rather than the deep plexus.

Vessel coarse irregularities, such as right-angle vessels, were particularly evident in eyes with concomitant pigment plaques (four eyes; 26.66%).

Since the introduction of the first classification system by Glass and Blodi,[2] and until recently, the gold standard for MacTel diagnosis was without a doubt FFA. Since, several imaging techniques have been used in MacTel and numerous imaging and multimodal imaging classifications have been proposed.[4–6]

In this study OCTA more clearly discerned some features of the diseases, such as vessel density, differential involvement of retinal plexuses, and retinal neovascularization, than did FFA. The observation of a more prominent ectasia of the deep vessels compared to that of the superficial vessels was in accordance with other authors investigating vessel density by means of OCTA.[7,13,14] The topographic sequence of vessel alterations detected by means of OCTA starting from the temporal retina was in accordance with the first observations of Gass and Oyakawa[1] and was related to the topographic succession of retinal alterations detected with other imaging techniques.[4,6,14]

Moreover, in accordance with previous studies we observed a rarefaction of vessel density.[7,14] The quantitative assessment of the vessel density by means of OCTA showed a reduction in vessel density, compared to that of age-matched normal

Table 10. Comparison of the Classification Determined With the Imaging Modalities Indicating the Spearman Correlation Coefficient and the *P* Corrected for Multiple Testing Using the False Discovery Rate

	FAF	Early FFA	Late FFA	SD-OCT	CBR	OCTA
FAF						
CC		0.667	0.667	0.824	0.453	0.759
P		0.007	0.007	0.000	0.090	0.002
Early FFA						
CC	0.667		1.000	0.745	0.680	0.775
P	0.007		0.000	0.002	0.006	0.002
Late FFA						
CC	0.667	1.000		0.745	0.680	0.775
P	0.007	0.000		0.002	0.006	0.002
SD-OCT						
CC	0.824	0.745	0.745		0.679	0.818
P	0.000	0.002	0.002		0.006	0.000
CBR						
CC	0.453	0.680	0.680	0.679		0.665
P	0.090	0.006	0.006	0.006		0.007
OCTA						
CC	0.759	0.775	0.775	0.818	0.665	
P	0.002	0.002	0.002	0.000	0.007	

Higher values of CC indicate a stronger correction and 1 indicates a perfect correlation. CC, correlation coefficient.

controls, which was significant for both the foveal superficial and deep plexus and for the superficial plexus in the parafoveal region.

These results were in accordance with those of Ziemer et al.[14] who found a loss of capillary density in the superficial plexus and enlargement of vessels and larger intervascular spaces in the deep plexus. In contrast, Spaide et al.[7] have found a loss of functional vessels, particularly in the deep plexus. In accordance with Spaide et al.,[7] we found a deep vessel rarefaction in the central 1-mm area (defined foveal region) but not in the parafoveal area (from 1–2.5 mm of diameter). These differences could be related in part to differences in the disease stage of the enrolled eyes. In fact, in the study of Spaide et al.,[7] 9 of 14 eyes (64%) are in an advanced proliferative stage of disease, while in our series only 20% of eyes were proliferative MacTel 2 eyes. Spaide et al.[7] have proposed that the vascular invasion occurs under, in the areas of more prominent retinal capillary loss.

This is the first objective evidence of reduced vessel density compared to that of normal eyes, not previously demonstrated either with FFA or with histologic assessment. It is known from recent studies based on multimodal imaging modalities that MacTel is considered a primary neurodegenerative disorder, with a pivotal role for Muller cell dysfunction and death in the disease process, as opposed to the first vascular theory proposed by Gass et al.[1,2] It is possible to hypothesize that vascular depletion could be a consequence of retinal neurodegeneration as proposed for vascular ectasia.

In our study OCTA showed a high correlation with FFA, thus demonstrating its validity in the diagnosis of MacTel, compared to the gold standard. A high correlation was also found with SD-OCT, a well-established imaging technique for demonstrating progressive neurodegenerative changes in MacTel. Optical coherence tomography angiography was superior to FFA in detecting neovascularization in our series as already evidenced by other authors.[15] The demonstration of a high correlation between OCTA and well-established imaging techniques used in the diagnosis of MacTel type 2 suggests the possible use of this noninvasive technique for early disease detection as well as for monitoring long-term vascular disease progression. The noninvasive nature of this imaging method allows for more frequent use than clinical angiography techniques currently used. Nevertheless, the high correlation of OCTA with other techniques is not sufficient to suggest it as a substitute for any other technique. This probably should not be considered a limitation of this technique, but rather a limit of its use based on canons derived from other techniques rather than on novel canons derived from the full potential of OCTA.

Potential limitations of this imaging method are related to difficulty in segmentation of retinal layers in diseased eyes and particularly with MacTel 2, in advanced stages with retinal atrophy, characterized by the collapse of retinal layers. In addition, poor fixation due to low vision in the more severe stages of this condition is linked to motion artifacts. The low number of diseased eyes examined was another study limitation. But this is due to it being a rare disease. More definite conclusions could be drawn with larger samples in multicenter studies.

Acknowledgments

Disclosure: **L. Toto**, None; **L. Di Antonio**, None; **R. Mastropasqua**, None; **P.A. Mattei**, None; **P. Carpineto**, None; **E. Borrelli**, None; **M. Rispoli**, None; **B. Lumbroso**, None; **L. Mastropasqua**, None

References

1. Gass JD, Oyakawa RT. Idiopathic juxtafoveolar retinal telangiectasis. *Arch Ophthalmol*. 1982;100:769–780.
2. Gass JD, Blodi BA. Idiopathic juxtafoveolar retinal telangiectasis: update of classification and follow-up study. *Ophthalmology*. 1993;100:1536–1546.
3. Yannuzzi LA, Bardal AM, Freund KB, et al. Idiopathic macular telangiectasia. *Arch Ophthalmol*. 2006;124:450–460.
4. Wu L, Evans T, Arevalo JF. Idiopathic macular telangiectasia type 2 (idiopathic juxtafoveolar retinal telangiectasis type 2A, Mac Tel 2). *Surv Ophthalmol*. 2013;58:536–559.
5. Wong WT, Forooghian F, Majumdar Z, Bonner RF, Cunningham D, Chew EY. Fundus autofluorescence in type 2 idiopathic macular telangiectasia: correlation with optical coherence tomography and microperimetry. *Am J Ophthalmol*. 2009; 148:573–583.
6. Sallo FB, Leung I, Clemons TE, Peto T, Bird AC, Pauleikhoff D. Multimodal imaging in type 2 idiopathic macular telangiectasia. *Retina*. 2015;35:742–749.
7. Spaide RF, Klancnik JM Jr, Cooney MJ. Retinal vascular layers imaged by fluorescein angiography and optical coherence tomography angiography. *JAMA Ophthalmol*. 2015;133:45–50.
8. Jia Y, Tan O, Tokayer J, et al. Split-spectrum amplitude decorrelation angiography with optical coherence tomography. *Opt Express*. 2012;20:4710–4725.
9. Jia Y, Morrison JC, Tokayer J, et al. Quantitative OCT angiography of optic nerve head blood flow. *Biomed Opt Express*. 2012;3:3127–3137.
10. Fingler J, Zawadzki RJ, Werner JS, Schwartz D, Fraser SE. Volumetric microvascular imaging of human retina using optical coherence tomography with a novel motion contrast technique. *Opt Express*. 2009;17:22190–22200.
11. Motaghiannezam SM, Koos D, Fraser SE. Differential phase-contrast, swept-source optical coherence tomography at 1060 nm for in vivo human retinal and choroidal vasculature visualization. *J Biomed Opt*. 2012;17:026011.

12. Mendis KR, Balaratnasingam C, Yu P, et al. Correlation of histologic and clinical images to determine the diagnostic value of fluorescein angiography for studying retinal capillary detail. *Invest Ophthalmol Vis Sci*. 2010;51:5864–5869.
13. Thorell MR, Zhang Q, Huang Y, et al. Swept-source OCT angiography of macular telangiectasia type 2. *Ophthalmic Surg Lasers Imaging Retina*. 2014;45:369–380.
14. Zeimer M, Gutfleisch M, Heimes B, Spital G, Lommatzsch A, Pauleikhoff D. Association between changes in macular vasculature in optical coherence tomography- and fluorescein-angiography and distribution of macular pigment in type 2 idiopathic macular telangiectasia. *Retina*. 2015;35:2307–2316.
15. Zhang Q, Wang RK, Chen CL, et al. Swept source optical coherence tomography angiography of neovascular macular telangiectasia type 2. *Retina*. 2015;35:2285–2299.
16. Gaudric A, Krivosic V, Tadayoni R. Outer retina capillary invasion and ellipsoid zone loss in macular telangiectasia type 2 imaged by optical coherence tomography angiography. *Retina*. 2015;35:2300–2306.

Investigative Ophthalmology & Visual Science